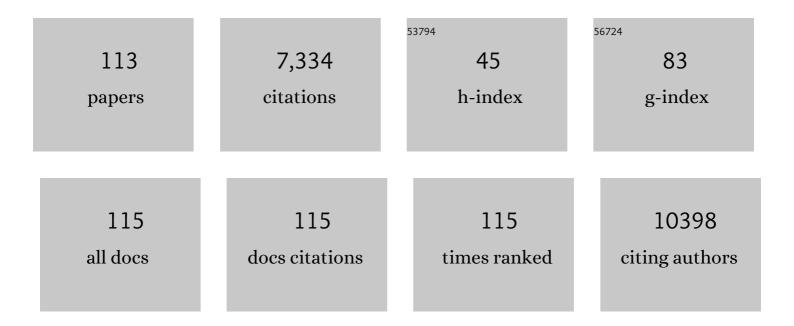
## Huimin Zhao

List of Publications by Year in descending order

Source: https://exaly.com/author-pdf/1893920/publications.pdf Version: 2024-02-01



Ηιμμινί Ζηλο

#	Article	IF	CITATIONS
1	Multiple application of SAzyme based on carbon nitride nanorod-supported Pt single-atom for H2O2 detection, antibiotic detection and antibacterial therapy. Chemical Engineering Journal, 2022, 427, 131572.	12.7	42
2	3D V2O5-MoS2/rGO nanocomposites with enhanced peroxidase mimicking activity for sensitive colorimetric determination of H2O2 and glucose. Spectrochimica Acta - Part A: Molecular and Biomolecular Spectroscopy, 2022, 269, 120750.	3.9	20
3	Recent advances and perspectives of enzyme-based optical biosensing for organophosphorus pesticides detection. Talanta, 2022, 240, 123145.	5.5	29
4	Sensitive detection of quorum signaling molecules ( <i>N</i> -acyl homoserine lactones) in activated sludge based on surface molecularly imprinted polymers on CQDs@MIL-101. Environmental Science: Water Research and Technology, 2022, 8, 1211-1222.	2.4	2
5	Adsorption performance and its mechanism of aqueous As (III) on polyporous calcined oyster shellâ€supported Feâ€Mn binary oxide. Water Environment Research, 2022, 94, e10714.	2.7	2
6	Enhanced Photocatalytic Production of H <sub>2</sub> O <sub>2</sub> through Regulation of Spatial Charge Transfer and Light Absorption over a MnIn <sub>2</sub> S <sub>4</sub> /WO <sub>3</sub> (Yb,) Tj ETQc	0 <b>6.⊅</b> rgB1	/Øøerlock 1
7	Activating the Basal Planes in 2Hâ€MoTe <sub>2</sub> Monolayers by Incorporating Singleâ€Atom Dispersed N or P for Enhanced Electrocatalytic Overall Water Splitting. Advanced Sustainable Systems, 2022, 6, .	5.3	4
8	Ultrasensitive sandwich-type photoelectrochemcial oxytetracycline sensing platform based on MnIn2S4/WO3 (Yb, Tm) functionalized rGO film. Journal of Electroanalytical Chemistry, 2022, 915, 116354.	3.8	1
9	Transition metal dichalcogenide-based mixed-dimensional heterostructures for visible-light-driven photocatalysis: Dimensionality and interface engineering. Nano Research, 2021, 14, 2003-2022.	10.4	61
10	Signal amplified sandwich-type photoelectrochemical sensing assay based on rGO-Znln2S4 functionalized Au–WO3 IOPCs Z-scheme heterojunction. Electrochimica Acta, 2021, 365, 137382.	5.2	10
11	Prevalence of antibiotic resistance genes in wastewater collected from ornamental fish market in northern China. Environmental Pollution, 2021, 271, 116316.	7.5	9
12	Catalytic hairpin assembly indirectly covalent on Fe3O4@C nanoparticles with signal amplification for intracellular detection of miRNA. Talanta, 2021, 223, 121675.	5.5	19
13	<scp>WO<sub>3</sub></scp> Inversce Opal Photonic Crystals: Unique Property, Synthetic Methods and Extensive Application. Chinese Journal of Chemistry, 2021, 39, 1706-1715.	4.9	8
14	2D Ti3C2Tx flakes prepared by in-situ HF etchant for simultaneous screening of carbamate pesticides. Journal of Colloid and Interface Science, 2021, 590, 365-374.	9.4	38
15	Highly sensitive detection of salvianic acid a drug by a novel electrochemical sensor based on HKUST-1 loaded on three-dimensional graphene-MWCNT composite. Journal of Pharmaceutical and Biomedical Analysis, 2021, 206, 114389.	2.8	5
16	Extending suitability of physisorption strategy in fluorescent platforms design: Surface passivation and covalent linkage on MOF nanosheets with enhanced OTC detection sensitivity. Sensors and Actuators B: Chemical, 2020, 303, 127230.	7.8	18
17	Selection and characterization of DNA aptamers for constructing colorimetric biosensor for detection of PBP2a. Spectrochimica Acta - Part A: Molecular and Biomolecular Spectroscopy, 2020, 228, 117735.	3.9	18
18	Bimetallic Fe/Mn metal-organic-frameworks and Au nanoparticles anchored carbon nanotubes as a peroxidase-like detection platform with increased active sites and enhanced electron transfer. Talanta, 2020, 210, 120678.	5.5	45

#	Article	IF	CITATIONS
19	Efficient visible-light activation of molecular oxygen to produce hydrogen peroxide using P doped g-C <sub>3</sub> N <sub>4</sub> hollow spheres. Journal of Materials Chemistry A, 2020, 8, 22720-22727.	10.3	59
20	Environmental and intercellular Pb2+ ions determination based on encapsulated DNAzyme in nanoscale metal-organic frameworks. Mikrochimica Acta, 2020, 187, 608.	5.0	14
21	Propagation of antibiotic resistance genes in an industrial recirculating aquaculture system located at northern China. Environmental Pollution, 2020, 261, 114155.	7.5	29
22	Signal amplified photoelectrochemical assay based on Polypyrrole/g-C3N4/WO3 inverse opal photonic crystals triple heterojunction assembled through sandwich-type recognition model. Sensors and Actuators B: Chemical, 2020, 310, 127888.	7.8	27
23	Preparation of 3D assembly of mono layered molybdenum disulfide nanotubules for rapid screening of carbamate pesticide diethofencarb. Talanta, 2019, 204, 455-464.	5.5	21
24	Enhanced Electrochemiluminescence Detection for Hydrogen Peroxide Using Peroxidase-Mimetic Fe/N-Doped Porous Carbon. Journal of the Electrochemical Society, 2019, 166, B1594-B1601.	2.9	16
25	CNT-Modified MIL-88(NH2)-Fe for Enhancing DNA-Regulated Peroxidase-Like Activity. Journal of Analysis and Testing, 2019, 3, 238-245.	5.1	7
26	A bimetallic Co/Mn metal–organic-framework with a synergistic catalytic effect as peroxidase for the colorimetric detection of H <sub>2</sub> 0 <sub>2</sub> . Analytical Methods, 2019, 11, 1111-1124.	2.7	60
27	Coupling O <sub>2</sub> and K <sub>2</sub> S <sub>2</sub> O <sub>8</sub> Dual Coâ€reactant with Feâ€N Modified Electrode for Ultrasensitive Electrochemiluminescence Signal Amplification. ChemistrySelect, 2019, 4, 1673-1680.	) 1.5	5
28	Electrochemical Preparation of Gold Nanoparticles-Polypyrrole Co-Decorated 2D MoS <sub>2</sub> Nanocomposite Sensor for Sensitive Detection of Glucose. Journal of the Electrochemical Society, 2019, 166, B147-B154.	2.9	48
29	Understanding signal amplification strategies of nanostructured electrochemical sensors for environmental pollutants. Current Opinion in Electrochemistry, 2019, 17, 56-64.	4.8	26
30	Three-Dimensional Branched Crystal Carbon Nitride with Enhanced Intrinsic Peroxidase-Like Activity: A Hypersensitive Platform for Colorimetric Detection. ACS Applied Materials & Interfaces, 2019, 11, 17467-17474.	8.0	29
31	Signal amplified photoelectrochemical sensing platform with g-C3N4/inverse opal photonic crystal WO3 heterojunction electrode. Journal of Electroanalytical Chemistry, 2019, 840, 101-108.	3.8	20
32	A strategy for enhancing anaerobic digestion of waste activated sludge: Driving anodic oxidation by adding nitrate into microbial electrolysis cell. Journal of Environmental Sciences, 2019, 81, 34-42.	6.1	8
33	Non enzymatic fluorometric determination of glucose by using quenchable g-C3N4 quantum dots. Mikrochimica Acta, 2019, 186, 779.	5.0	10
34	Real Time Detection of Hazardous Hydroxyl Radical Using an Electrochemical Approach. ChemistrySelect, 2019, 4, 12507-12511.	1.5	14
35	Developmental perfluorooctane sulfonate exposure inhibits long-term potentiation by affecting AMPA receptor trafficking. Toxicology, 2019, 412, 55-62.	4.2	10
36	Covalent functionalization of MoS2 nanosheets synthesized by liquid phase exfoliation to construct electrochemical sensors for Cd (II) detection. Talanta, 2018, 182, 38-48.	5.5	58

#	Article	IF	CITATIONS
37	Enhanced adsorption of ionizable antibiotics on activated carbon fiber under electrochemical assistance in continuous-flow modes. Water Research, 2018, 134, 162-169.	11.3	47
38	MoS2 nanostructures for electrochemical sensing of multidisciplinary targets: A review. TrAC - Trends in Analytical Chemistry, 2018, 102, 75-90.	11.4	138
39	Voltammetric sensing based on the use of advanced carbonaceous nanomaterials: a review. Mikrochimica Acta, 2018, 185, 89.	5.0	67
40	Facile Ammonia Synthesis from Electrocatalytic N <sub>2</sub> Reduction under Ambient Conditions on N-Doped Porous Carbon. ACS Catalysis, 2018, 8, 1186-1191.	11.2	520
41	Enhancing nitrogen removal efficiency in a dyestuff wastewater treatment plant with the IFFAS process: the pilot-scale and full-scale studies. Water Science and Technology, 2018, 77, 70-78.	2.5	7
42	Roles of magnetite and granular activated carbon in improvement of anaerobic sludge digestion. Bioresource Technology, 2018, 249, 666-672.	9.6	163
43	Amphiphilic PA-induced three-dimensional graphene macrostructure with enhanced removal of heavy metal ions. Journal of Colloid and Interface Science, 2018, 512, 853-861.	9.4	47
44	Electrochemical Oxidation of Tannic Acid at ZIF-8 Induced Nitrogen Doped Porous Carbon Nanoframework Modified Electrode. Journal of the Electrochemical Society, 2018, 165, H1004-H1011.	2.9	9
45	Two-dimensional nanomaterial based sensors for heavy metal ions. Mikrochimica Acta, 2018, 185, 478.	5.0	48
46	Enhanced photocatalytic performance of a two-dimensional BiOIO3/g-C3N4 heterostructured composite with a Z-scheme configuration. Applied Catalysis B: Environmental, 2018, 237, 947-956.	20.2	99
47	Photoelectrochemical aptasensor for sulfadimethoxine using g-C3N4 quantum dots modified with reduced graphene oxide. Mikrochimica Acta, 2018, 185, 345.	5.0	38
48	Two-dimensional MoS2: A promising building block for biosensors. Biosensors and Bioelectronics, 2017, 89, 56-71.	10.1	215
49	Determination of Oxytetracycline by a Graphene—Gold Nanoparticle-Based Colorimetric Aptamer Sensor. Analytical Letters, 2017, 50, 544-553.	1.8	26
50	Poly(vinylidene fluoride) hollowâ€fiber membranes containing silver/graphene oxide dope with excellent filtration performance. Journal of Applied Polymer Science, 2017, 134, .	2.6	21
51	PECylated molybdenum dichalcogenide (PEG-MoS <sub>2</sub> ) nanosheets with enhanced peroxidase-like activity for the colorimetric detection of H <sub>2</sub> O <sub>2</sub> . New Journal of Chemistry, 2017, 41, 6700-6708.	2.8	42
52	A colorimetric aptasensor for sulfadimethoxine detection based on peroxidase-like activity of graphene/nickel@palladium hybrids. Analytical Biochemistry, 2017, 525, 92-99.	2.4	46
53	Selective Electrochemical Reduction of Carbon Dioxide to Ethanol on a Boron―and Nitrogenâ€Coâ€doped Nanodiamond. Angewandte Chemie, 2017, 129, 15813-15817.	2.0	196
54	Selective Electrochemical Reduction of Carbon Dioxide to Ethanol on a Boron―and Nitrogenâ€Coâ€doped Nanodiamond. Angewandte Chemie - International Edition, 2017, 56, 15607-15611.	13.8	226

#	Article	IF	CITATIONS
55	Innentitelbild: Selective Electrochemical Reduction of Carbon Dioxide to Ethanol on a Boron―and Nitrogenâ€Coâ€doped Nanodiamond (Angew. Chem. 49/2017). Angewandte Chemie, 2017, 129, 15678-15678.	2.0	1
56	Fe <sub>3</sub> O <sub>4</sub> -AuNPs anchored 2D metal–organic framework nanosheets with DNA regulated switchable peroxidase-like activity. Nanoscale, 2017, 9, 18699-18710.	5.6	122
57	Enhancement of anaerobic methanogenesis at a short hydraulic retention time via bioelectrochemical enrichment of hydrogenotrophic methanogens. Bioresource Technology, 2016, 218, 505-511.	9.6	66
58	Developmental perfluorooctane sulfonate exposure results in tau hyperphosphorylation and β-amyloid aggregation in adults rats: Incidence for link to Alzheimer's disease. Toxicology, 2016, 347-349, 40-46.	4.2	18
59	Three-Dimensional Graphene Supported Bimetallic Nanocomposites with DNA Regulated-Flexibly Switchable Peroxidase-Like Activity. ACS Applied Materials & Interfaces, 2016, 8, 9855-9864.	8.0	89
60	A versatile fluorescent biosensor based on target-responsive graphene oxide hydrogel for antibiotic detection. Biosensors and Bioelectronics, 2016, 83, 267-273.	10.1	123
61	Electrochemical reduction of carbon dioxide to formate with Fe-C electrodes in anaerobic sludge digestion process. Water Research, 2016, 106, 339-343.	11.3	37
62	Dynamic adsorption of ciprofloxacin on carbon nanofibers: Quantitative measurement by in situ fluorescence. Journal of Water Process Engineering, 2016, 9, e14-e20.	5.6	61
63	Enhancement of sludge granulation in hydrolytic acidogenesis by denitrification. Applied Microbiology and Biotechnology, 2016, 100, 3313-3320.	3.6	14
64	A visible and label-free colorimetric sensor for miRNA-21 detection based on peroxidase-like activity of graphene/gold-nanoparticle hybrids. Analytical Methods, 2016, 8, 2005-2012.	2.7	57
65	Effects of perfluorooctane sulfonate and its alternatives on long-term potentiation in the hippocampus CA1 region of adult rats in vivo. Toxicology Research, 2016, 5, 539-546.	2.1	35
66	An Electrochemical Sensor based on p-aminothiophenol/Au Nanoparticle-Decorated H TiS2 Nanosheets for Specific Detection of Picomolar Cu (II). Electrochimica Acta, 2016, 190, 480-489.	5.2	18
67	Nanocarbon-based membrane filtration integrated with electric field driving for effective membrane fouling mitigation. Water Research, 2016, 88, 285-292.	11.3	89
68	Evaluation on direct interspecies electron transfer in anaerobic sludge digestion of microbial electrolysis cell. Bioresource Technology, 2016, 200, 235-244.	9.6	157
69	Three-Dimensional Porous H <sub><i>x</i></sub> TiS <sub>2</sub> Nanosheet–Polyaniline Nanocomposite Electrodes for Directly Detecting Trace Cu(II) Ions. Analytical Chemistry, 2015, 87, 5605-5613.	6.5	39
70	Fluorescent biosensor for sensitive analysis of oxytetracycline based on an indirectly labelled long-chain aptamer. RSC Advances, 2015, 5, 58895-58901.	3.6	32
71	Visible assay for glycosylase based on intrinsic catalytic ability of graphene/gold nanoparticles hybrids. Biosensors and Bioelectronics, 2015, 68, 7-13.	10.1	37
72	Effects of developmental perfluorooctane sulfonate exposure on spatial learning and memory ability of rats and mechanism associated with synaptic plasticity. Food and Chemical Toxicology, 2015, 76, 70-76.	3.6	54

#	Article	IF	CITATIONS
73	An electrochemical sensor for selective determination of sulfamethoxazole in surface water using a molecularly imprinted polymer modified BDD electrode. Analytical Methods, 2015, 7, 2693-2698.	2.7	50
74	Photochemical Formation of Hydroxylated Polybrominated Diphenyl Ethers (OH-PBDEs) from Polybrominated Diphenyl Ethers (PBDEs) in Aqueous Solution under Simulated Solar Light Irradiation. Environmental Science & Technology, 2015, 49, 9092-9099.	10.0	35
75	Perfluorooctane sulfonate induces apoptosis of hippocampal neurons in rat offspring associated with calcium overload. Toxicology Research, 2015, 4, 931-938.	2.1	12
76	Voltage-Gated Transport of Nanoparticles across Free-Standing All-Carbon-Nanotube-Based Hollow-Fiber Membranes. ACS Applied Materials & Interfaces, 2015, 7, 14620-14627.	8.0	14
77	DNA-modified graphene quantum dots as a sensing platform for detection of Hg <sup>2+</sup> in living cells. RSC Advances, 2015, 5, 39587-39591.	3.6	43
78	Improved Photocatalytic Performance of Heterojunction by Controlling the Contact Facet: High Electron Transfer Capacity between TiO <sub>2</sub> and the {110} Facet of BiVO <sub>4</sub> Caused by Suitable Energy Band Alignment. Advanced Functional Materials, 2015, 25, 3074-3080.	14.9	164
79	Efficient Mineralization of Perfluorooctanoate by Electro-Fenton with H <sub>2</sub> O <sub>2</sub> Electro-generated on Hierarchically Porous Carbon. Environmental Science & Technology, 2015, 49, 13528-13533.	10.0	174
80	Impact of dissolved organic matter on the photolysis of the ionizable antibiotic norfloxacin. Journal of Environmental Sciences, 2015, 27, 115-123.	6.1	50
81	Reduction of acute toxicity and genotoxicity of dye effluent using Fenton-coagulation process. Journal of Hazardous Materials, 2014, 274, 198-204.	12.4	54
82	Atomic single layer graphitic-C <sub>3</sub> N <sub>4</sub> : fabrication and its high photocatalytic performance under visible light irradiation. RSC Advances, 2014, 4, 624-628.	3.6	152
83	Ultrasensitive immunoassay of microcystins-LR using G-quadruplex DNAzyme as an electrocatalyst. International Journal of Environmental Analytical Chemistry, 2014, 94, 988-1000.	3.3	9
84	Porous metal–organic framework MIL-100(Fe) as an efficient catalyst for the selective catalytic reduction of NO <sub>x</sub> with NH <sub>3</sub> . RSC Advances, 2014, 4, 48912-48919.	3.6	80
85	A ZIF-8-based platform for the rapid and highly sensitive detection of indoor formaldehyde. RSC Advances, 2014, 4, 36444-36450.	3.6	26
86	Electrochemically enhanced adsorption of PFOA and PFOS on multiwalled carbon nanotubes in continuous flow mode. Science Bulletin, 2014, 59, 2890-2897.	1.7	17
87	Photochemical transformation of 2,2′,4,4′-tetrabromodiphenyl ether (BDE-47) in surface coastal waters: Effects of chloride and ferric ions. Marine Pollution Bulletin, 2014, 86, 76-83.	5.0	23
88	Fabrication of atomic single layer graphitic-C3N4 and its high performance of photocatalytic disinfection under visible light irradiation. Applied Catalysis B: Environmental, 2014, 152-153, 46-50.	20.2	394
89	Electrochemical Biosensor for Detection of Perfluorooctane Sulfonate Based on Inhibition Biocatalysis of Enzymatic Fuel Cell. Electrochemistry, 2014, 82, 94-99.	1.4	22
90	Fluorescent assay for oxytetracycline based on a long-chain aptamer assembled onto reduced graphene oxide. Mikrochimica Acta, 2013, 180, 829-835.	5.0	57

#	Article	IF	CITATIONS
91	A graphene and multienzyme functionalized carbon nanosphere-based electrochemical immunosensor for microcystin-LR detection. Colloids and Surfaces B: Biointerfaces, 2013, 103, 38-44.	5.0	44
92	Boron and Nitrogen Codoped Nanodiamond as an Efficient Metal-Free Catalyst for Oxygen Reduction Reaction. Journal of Physical Chemistry C, 2013, 117, 14992-14998.	3.1	80
93	Tuning the electrochemical properties of a boron and nitrogen codoped nanodiamond rod array to achieve high performance for both electro-oxidation and electro-reduction. Journal of Materials Chemistry A, 2013, 1, 14706.	10.3	16
94	A universal immunosensing strategy based on regulation of the interaction between graphene and graphene quantum dots. Chemical Communications, 2013, 49, 234-236.	4.1	156
95	Graphene oxide modified g-C <sub>3</sub> N <sub>4</sub> hybrid with enhanced photocatalytic capability under visible light irradiation. Journal of Materials Chemistry, 2012, 22, 2721-2726.	6.7	687
96	Photoelectrochemical immunoassay for microcystin-LR based on a fluorine-doped tin oxide glass electrode modified with a CdS-graphene composite. Mikrochimica Acta, 2012, 179, 163-170.	5.0	39
97	Stimuli-responsive peroxidase mimicking at a smart graphene interface. Chemical Communications, 2012, 48, 7055.	4.1	76
98	Interface Engineering Catalytic Graphene for Smart Colorimetric Biosensing. ACS Nano, 2012, 6, 3142-3151.	14.6	270
99	Gold modified microelectrode for direct tetracycline detection. Frontiers of Environmental Science and Engineering, 2012, 6, 313-319.	6.0	23
100	Enhanced photocatalytic degradation of tetracycline hydrochloride by molecular imprinted film modified TiO2 nanotubes. Science Bulletin, 2012, 57, 601-605.	1.7	30
101	Salt-controlled assembly of stacked-graphene for capturing fluorescence and its application in chemical genotoxicity screening. Journal of Materials Chemistry, 2011, 21, 15266.	6.7	6
102	Controllable oxidative DNA cleavage-dependent regulation of graphene/DNA interaction. Chemical Communications, 2011, 47, 4084.	4.1	50
103	In situ controllable growth of noble metal nanodot on graphene sheet. Journal of Materials Chemistry, 2011, 21, 12986.	6.7	36
104	Electrochemical Determination of Tetracycline Using Molecularly Imprinted Polymer Modified Carbon Nanotubeâ€Gold Nanoparticles Electrode. Electroanalysis, 2011, 23, 1863-1869.	2.9	77
105	Influence of Temperature and Oil Content on the Soil/Air Partition Coefficient for Hexachlorobenzene in Oil-Contaminated Rice Paddy Field Soil. Soil and Sediment Contamination, 2011, 20, 221-233.	1.9	1
106	Electrocatalytic dechlorination of 2,4,5-trichlorobiphenyl using an aligned carbon nanotubes electrode deposited with palladium nanoparticles. Science Bulletin, 2010, 55, 358-364.	1.7	8
107	Facile Method for Fabricating Boron-Doped TiO <sub>2</sub> Nanotube Array with Enhanced Photoelectrocatalytic Properties. Industrial & Engineering Chemistry Research, 2008, 47, 3804-3808.	3.7	107
108	Enhanced Photodegradation of PNP on Soil Surface under UV Irradiation with TiO2. Soil and Sediment Contamination, 2007, 16, 413-421.	1.9	16

#	Article	IF	CITATIONS
109	TiO <sub>2</sub> â^'Multiwalled Carbon Nanotube Heterojunction Arrays and Their Charge Separation Capability. Journal of Physical Chemistry C, 2007, 111, 12987-12991.	3.1	222
110	Fabrication of needle-like ZnO nanorods arrays by a low-temperature seed-layer growth approach in solution. Applied Physics A: Materials Science and Processing, 2007, 89, 673-679.	2.3	11
111	Preparation of Zn-doped TiO2 nanotubes electrode and its application in pentachlorophenol photoelectrocatalytic degradation. Science Bulletin, 2007, 52, 1456-1461.	1.7	52
112	Degradation of p-nitrophenol in aqueous solution by microwave assisted oxidation process through a granular activated carbon fixed bed. Water Research, 2006, 40, 3061-3068.	11.3	114
113	Preparation and characterization of aligned carbon nanotubes coated with titania nanoparticles. Science Bulletin, 2006, 51, 2294-2296.	1.7	14